

Simplification of Robotic System Model Analysis by Petri Net Meta-Model Property Transfer

Maksym Figat*, *Member, IEEE* and Cezary Zieliński, *Senior Member, IEEE*

Abstract—This paper presents a simplification of robotic system model analysis due to the transfer of Robotic System Hierarchical Petri Net (RSHPN) meta-model properties onto the model of a designed system. Key contributions include: 1) analysis of RSHPN meta-model properties; 2) decomposition of RSHPN analysis into analysis of individual Petri nets, thus the reduction of state space explosion; and 3) transfer of RSHPN meta-model properties onto the produced models, hence elimination of the need for full re-analysis of the RSHPN model when creating new robotic systems. Only task-dependent parts of the model need to be analyzed. This approach streamlines the analysis thus reducing the design time. Moreover, it produces a specification which is a solid foundation for the implementation of the system. The obtained results highlight the potential of Petri nets as a valuable formal framework for analyzing robotic system properties.

Index Terms—Robotic system design, Hierarchical Petri Net, Robotic system meta-model, Model analysis

I. INTRODUCTION

As robots ever more often execute complex tasks in close proximity of humans, the need for their accurate and safe operation is crucial. However, formal methods for system description, a vital component of model-based approaches, are often overlooked, thus flaws are detected as late as the implementation or even verification stages, hence resulting in costly redesigns [1]. Component-based development frameworks, e.g. ROS, offer flexibility, but lack stringent guidelines, what makes the quality of the resulting systems heavily dependent on the designer’s experience, often leading to inferior software code [2]. The quality of such systems can be verified at the runtime verification stage, i.e. there are many ROS-based tools for analysis, e.g. SOTER [3], ROSMonitoring [4], ROSRV [5]. However, they are mainly used to analyse the message flow between nodes that are treated as black boxes, so it is not possible to analyse the state of subsystems directly, which makes it much more difficult to perform an overall analysis of the designed system and significantly narrows the potential space of analysed properties, as stated in [6]. Utilisation of formal methods could greatly improve system reliability and safety, thus minimizing risks and redesign expenses.

Formal methods are necessary to perform model (i.e. specification) checking before implementation. They play a crucial role in model-based design methods, enabling system specification [7] and analysis, though their application to robotics is a

challenge [2]. Many model-based approaches focus on specific robot tasks (multi-robot path planning [8], [9]) or even layers (decision layer [10], functional layer [6]), without providing a holistic view of the system. Moreover, a predominant focus on implementation, sidelining specification, even in many model-driven engineering approaches, couples modelling and implementation concepts, hindering the development of platform-independent models and comprehensive system analysis [2].

Lack of formal system model prior to implementation is usually due to: (a) computational complexity of the analysis [11], (b) scalability problems in model checking [6], and (c) explosion of the state space (as in a variable structure multi-robot system modelled by Variable Petri net (VPN) [11]). Decomposition of the analysis is seen as a remedy to the problem of excessive model complexity [12], however in this particular case the analysed system was rudimentary, limited to motion planning for simple robots in a fixed structure environment. To mitigate state space explosion runtime verification (RV) is performed. RV does not require a model of the system, but this limits the class of properties that can be analysed. Nevertheless, by adding to RV a model of the system, treated as *a priori* knowledge, predictive RV is obtained [13], [14]. Future system states are predicted. However, this is still done after the implementation phase.

We developed a parametric Robotic System Hierarchical Petri Net (RSHPN) meta-model [15]. The six-layered RSHPN models the activity of the entire robotic system. Parameters derived from robotics ontology define both the structure and the activities of the system and its components. Domain-specific Robotic System Specification Language (RSSL) [16] is used to define the RSHPN parameters thus transforming the meta-model into a model. The model is used to generate the controller code and perform the analysis. This forms the Robotic System Design Methodology (RSDM) [17]¹.

Conventional Petri net (PN) analysis tools (e.g. Tina [18]) applied to RSHPN were of limited utility, even for a simple robot [15] (due to state space explosion resulting from the requirement of analysing a flat PN). A PN with 1168 places, 1294 transitions and 3085 edges produced a reachability graph of over 25 million nodes and 163 million edges. A 32 GB RAM computer did not cope. For more complex systems, e.g. multi-robot systems with dynamic structure [19], the situation would only be aggravated. Thus, an alternative method for analysing RSHPN was devised. This paper shows that the RSHPN structure greatly simplifies the designed system

Maksym Figat and Cezary Zieliński are with Warsaw University of Technology, Institute of Control and Computation Engineering, Warsaw, Poland.
*Corresponding author: Maksym Figat (maksym.figat@pw.edu.pl)

This work has been submitted to the IEEE for possible publication. Copyright may be transferred without notice, after which this version may no longer be accessible.

¹Introduction to the RSDM: <https://youtu.be/027JvJ-CtjY>

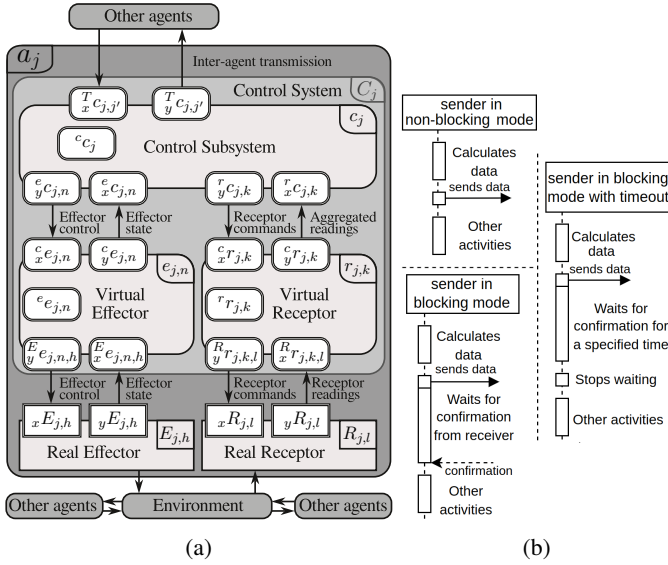


Fig. 1: (a): Structure of an embodied agent; (b): 3 communication modes from the perspective of the sending subsystem

analysis due to hierarchical decomposition (video tutorial²).

Our contribution is: 1) Analysis of selected properties of RSHPN meta-model, based on its intrinsic structure; 2) Decomposition of RSHPN analysis into analysis of individual PNs, reducing state space explosion; 3) Preservation of the RSHPN meta-model properties in each produced RSHPN model – full re-analysis of the RSHPN model is unnecessary. It is sufficient to analyze only the parts of the model that depend on the task and communication between subsystems.

The following presents: Sec. II – introduction to the robotic system architecture based on embodied agents, Sec. III – introduction to PNs, Sec. IV – RSHPN meta-model, Sec V – RSHPN meta-model analysis, Sec. VI – analysis results, Sec. VII – case study based on exemplary robotic system, Sec. VIII – discussion, and Sec. IX – conclusions.

II. ROBOTIC SYSTEM ARCHITECTURE

Structure of a robotic system: A robotic system \mathcal{RS} consists of one or more robots and auxiliary devices. Each robot consists of one or more embodied agents [15]. An embodied agent a_j (Fig. 1a) consists of: a single control subsystem c_j , real receptors $R_{j,l}$, real effectors $E_{j,h}$, virtual effectors $e_{j,n}$, and virtual receptors $r_{j,k}$. Tab. I provides the description of the notation used. Receptors $R_{j,l}$ collect data from the environment and pass it to $r_{j,k}$ to be aggregated and subsequently sent to c_j . Based on this data and the task, c_j produces control commands for $e_{j,n}$, which in turn transforms them to affect the environment via $E_{j,h}$. Subsystems share a common structure. Each subsystem $s_{j,v}$ of an agent a_j contains: 1) $^s s_{j,v}$ (internal memory), 2) input buffers $x^s \hat{s}_{j,v}$ and 3) output buffers $y^s \hat{s}_{j,v}$ (where \hat{X} is a set of X).

Activity of a robotic system: A robotic system task \mathcal{T} is composed of the tasks \mathcal{T}_j executed by the agents a_j , and those are composed of tasks $\mathcal{T}_{j,v}$ executed by subsystems

TABLE I: Robotic System Architecture notation

central symbol
types of subsystems \rightarrow \boxed{s} \leftarrow discrete time or type of function
list of substitutes for names, e.g.: $j, v, \omega, k, n, l, h, \alpha, \xi, \beta, \gamma, \psi, \phi$
input/output designators: x, y

Structure:		Activity:	
Central symbol	Description	Central symbol	Description
a	agent	\mathcal{T}	task
C	control system	\mathcal{B}	behaviour
E	real effector	f	transition function
R	real receptor	f^σ	initial condition
s	subsystem	f^τ	terminal condition
c	control subsystem	f^ϵ	error condition
e	virtual effector	aa	inter-agent channel
r	virtual receptor	ss	intra-agent channel
List of names	Description	List of names	Description
j, j'	names of agents	α	name of initial condition
v, v'	names of subsystems	ξ	name of terminal condition
k	name of virtual receptor	β	name of error condition
n	name of virtual effector	γ	name of transition function
l	name of real receptor	ψ	name of partial function
h	name of real effector	ϕ	name of overloaded function
v	subsystem name	ω, ω'	names of behaviours

$s_{j,v}$. Subsystem tasks $\mathcal{T}_{j,v}$ are executed by selecting specific behaviours $^s \mathcal{B}_{j,v,\omega}$. The specific behaviour to be executed is selected by testing its initial condition $^s f_{j,v,\alpha}^\sigma$ (α – predicate designator) [15]. Each behaviour iteratively: 1) Calculates the associated transition function $^s f_{j,v,\gamma}$, which takes as arguments the data from internal memory $^s s_{j,v}^l$ and input buffers $x^s \hat{s}_{j,v}^l$, and inserts the calculated results into the output buffers $y^s \hat{s}_{j,v}^{l+1}$ and the internal memory $^s s_{j,v}^{l+1}$, where l is the current time instant and $l+1$ is the next time instant: $(^s s_{j,v}^{l+1}, y^s \hat{s}_{j,v}^{l+1}) := ^s f_{j,v,\gamma}(^s s_{j,v}^l, x^s \hat{s}_{j,v}^l)$, 2) Sends data from the output buffers $y^s \hat{s}_{j,v}^{l+1}$ to the associated subsystems, 3) Increments the discrete time counter l , 4) Receives data from the associated subsystems and inserts it into input buffers $x^s \hat{s}_{j,v}^l$, and 5) Checks the terminal $^s f_{j,v,\xi}^\tau$ and error $^s f_{j,v,\beta}^\epsilon$ conditions. Behaviour $^s \mathcal{B}_{j,v,\omega}$ terminates when one of those conditions is fulfilled. In such a case the $s_{j,v}$ selects the next behaviour, e.g. $^s \mathcal{B}_{j,v,\omega'}$ based on the fulfilled initial condition $^s f_{j,v,(\omega,\omega')}^\sigma$ defined by the subsystem task $\mathcal{T}_{j,v}$.

Two subsystems, $s_{j,v}$ and $s_{j,h}$, can communicate, each using one of three modes: 1) blocking, 2) blocking with timeout, or 3) non-blocking mode (resulting in 9 possible communication models) [15], [20]. In blocking mode $s_{j,v}$ waits for $s_{j,h}$ to acknowledge receiving data, while in non-blocking mode, $s_{j,v}$ continues its activities after sending data, as presented in Fig. 1b. In blocking mode $s_{j,h}$ waits for data, while in non-blocking mode it continues its tasks even if data is not available.

III. PETRI NET PRELIMINARIES

A. Petri Net (PN)

PN is a bipartite graph with two kinds of nodes: places p (single circles) and transitions t (rectangles). Directed arcs connect places to transitions and vice versa. PNs are represented either graphically (e.g. Fig. 2) or algebraically. Evolution of PN marking represents the changes of system

²RSHPN analysis video: <https://youtu.be/JenAB1IKVVY>

state. $\mu(p_i)$ indicates marking, i.e. number of tokens (filled-in black circles) in a place $p_i \in \hat{p}$, where $\mu(p_i) \geq 0$ and \hat{p} is a set of places; M_m is a PN marking vector in instant m , $M_m = (\mu^m(p_1), \dots, \mu^m(p_k))^\top$, where $k = |\hat{p}|$ and $m \geq 0$ (in general $|\hat{x}|$ is the cardinality of set \hat{x}); M_0 indicates the initial marking and M_m marking m derived from M_0 ; $M_m(p_i)$ is the number of tokens in place p_i while in M_m . PN in an algebraic form is represented by the incidence matrix. For a PN with $|\hat{t}|$ transitions and $|\hat{p}|$ places, the incidence matrix $N = [n_{ij}]$ is a $|\hat{t}| \times |\hat{p}|$ matrix containing integers; n_{ij} represents the change of the number of tokens in a place p_j when $t_i \in \hat{t}$ fires [21]:

$$n_{ij} = n_{ij}^+ - n_{ij}^- \quad (1)$$

n_{ij}^- denotes the number of tokens removed from the input place p_j and n_{ij}^+ denotes the number of tokens inserted into p_j , both after firing t_i . If for $M_m \forall p_j (n_{ij}^- \leq M_m(p_j))$, then t_i fires causing a transition: $M_m \xrightarrow{t_i} M_{m+1}$. The marking M_m is a column vector $|\hat{p}| \times 1$. As the i -th row in the incidence matrix N denotes the change in the marking from M_m to the marking M_{m+1} as a result of firing t_i , the new marking of the network can be expressed by the formula Eq. (2).

$$M_{m+1} = M_m + N^\top \cdot u_{m+1} \quad (2)$$

where u_{m+1} is a column vector $|\hat{t}| \times 1$ containing 1 at position i (denoting the firing of t_i) with 0 at all other positions. Thus:

$$M_m - M_0 = N^\top \cdot (u_1 + \dots + u_m) = N^\top \cdot \mathbf{x} \quad (3)$$

where \mathbf{x} (called firing count vector [21]) is a column vector of dimension $|\hat{t}| \times 1$ with non-negative integer values, where i -th value in the vector \mathbf{x} denotes the number of times the transition t_i fires, leading from M_0 to M_m , i.e. $M_0 \xrightarrow{\mathbf{x}} M_m$.

B. Hierarchical Petri Net (HPN)

Hierarchical Petri Net (HPN) \mathcal{H} [15], [20] extends a PN by introducing pages \mathcal{P} (double circles) representing an underlying PN (rectangular panel connected by a dashed arrow to its page – Table II). Each such net has a single input p^{in} and a single output p^{out} place. When the token appears within page \mathcal{P} , it appears in the input place of the lower level PN (token “drops” down), and the lower PN is activated. When its activity is finished then the token appears within the output place p^{out} (token “jumps up” to the page), and becomes visible to the PN containing the page. Logical conditions \mathcal{C} and priorities $\mathcal{P}r$ are associated with transitions, and operations \mathcal{O} with places.

C. Place and transition invariants

Invariants [21], [23] are properties of the logical structure of a network. They characterize the way transitions are fired [22].

Place invariants express properties of reachable markings [23], i.e. they describe sets of places in PN where the weighted sum of tokens for each reachable marking remains constant. Let \mathbf{y} be the vector of weights assigned to places for which the assumption of place invariants is satisfied. This is equivalent to: $M_m^\top \cdot \mathbf{y} = M_0^\top \cdot \mathbf{y} = \text{const}$, i.e.: $(M_m - M_0)^\top \cdot \mathbf{y} = \mathbf{0}$, and by using Eq. (3) we obtain:

$$\mathbf{x}^\top \cdot (N \cdot \mathbf{y}) = \mathbf{0}, \text{ and since } \mathbf{x} \neq \mathbf{0} \text{ then: } N \cdot \mathbf{y} = \mathbf{0} \quad (4)$$

TABLE II: RSHPN notation [15]

Notation of RSHPN concepts			Graphical notation	
Central symbol	Description	Substitutes	Keyword	Description
p	place	j	in	input place
\mathcal{P}	page	v	out	output place
t	transition	ω	\mathcal{B}	behaviour layer
\mathcal{H}	hierarchical Petri net	ψ	snd	send sublayer
\mathcal{C}	condition	ρ	rcv	receive sublayer
a	agent	κ	fusion	fused place
s	subsystem		f	transition function sublayer

The solutions of Eq. (4) for $\mathbf{y} \neq \mathbf{0}$ are called place invariants (guaranteeing constant weighted sum of tokens). The set of places corresponding to non-zero elements of the solution is $\|\mathbf{y}\|$, called the support of place invariant [21]. Firing any transition in PN does not change the weighted sum of tokens from $\|\mathbf{y}\|$. This enables distinction of the set of places representing operations repeated cyclically and those dependent on each other. For example, if the sum of tokens is 1, then only one operation is executed from those represented by the places in $\|\mathbf{y}\|$. By obtaining two independent vectors \mathbf{y}_1 and \mathbf{y}_2 , one can observe parallel operations, such as those performed by two simultaneously operating subsystems.

Transition invariants are vectors defining the number of transition firings keeping the marking of PN the same, i.e. after firing transitions as many times as specified in the transition invariant vector, PN will switch from M_0 to M_m , but $M_m = M_0$. Hence, based on Eq. (3) we obtain $N^\top \cdot \mathbf{x} = \mathbf{0}$. The non-zero solutions of this equation are transition invariants. The set of transitions corresponding to the non-zero elements of the solution is $\|\mathbf{x}\|$, called the support of transition invariant [21], i.e. firing all transitions from $\|\mathbf{x}\|$ does not change PN marking, e.g. if $\mathbf{x} = (1, 2)^\top$ and PN starts from M_0 it will reach M_0 by firing: t_1 once and t_2 twice, i.e. $M_0 \xrightarrow{(t_1), (t_2)^2} M_0$. The transition invariant does not specify the order of transition firings. Transition invariants can be used to prove the repeatability of the system and the absence of deadlocks while firing transitions from $\|\mathbf{x}\|$.

D. Selected PN properties to be analysed

PN is deadlock-free: if for any reachable marking M_m (i.e. derived from M_0) there is always at least one fireable transition (i.e. enabled with a fulfilled condition). Absence of global deadlock in \mathcal{H} does not imply local deadlock cannot occur in any subsystem or between communicating subsystems. Therefore, individual lower level PNs need to be analysed.

PN is safe: if for any reachable marking M_m each place p_i contains at the most one token, i.e. $0 \leq M_m(p_i) \leq 1$. Safety assures that the operation associated with the place p_i cannot be executed concurrently to itself.

PN is conservative: [21] if $\forall p_i \in \hat{p} \mathbf{y}(p_i) > 0$ the weighted sum of tokens for every reachable marking M_m is constant, i.e.: $\sum_{p_i \in \hat{p}} \mathbf{y}(p_i) \cdot M_m(p_i) = \sum_{p_i \in \hat{p}} \mathbf{y}(p_i) \cdot M_0(p_i) = \text{const}$. If $\mathbf{y}(p_i) \geq 0$ and $\mathbf{y} \neq \mathbf{0}$ then PN is **partially conservative**,

while if $\mathbf{y} = (1, \dots, 1)^T$ then PN is **strictly conservative**, i.e. the number of tokens in PN remains the same for any M_m .

E. Methods of HPN analysis

Analysis of a HPN requires its decomposition into separate PNs. Each such PN needs modifications: (a) replacing a higher-level network with a transition connecting its output to the input place, and (b) replacing pages with places. This modification is valid only if the lower-layer PNs satisfy the property; the HPN fulfills the property if the modified PN and all its lower-layer PNs do. These modifications follow the reduction methods outlined in [21]. Then, properties of individual networks are analyzed using one of three methods: 1) PN interpretation, 2) reachability graph construction, or 3) place/transition invariants analysis. The choice of method depends on the complexity of the network being analyzed.

Petri net interpretation: It consists in firing enabled transitions and presenting graphically all possible markings M_m that can be derived from M_0 , as shown in Fig. 4 and Fig. 5.

Reachability graph analysis: Reachability graph nodes represent markings M_m derived from M_0 , while edges show transformations of markings due to firing transitions t , e.g. $M_0 \rightarrow \dots \rightarrow M_m \xrightarrow{t} M_{m+1}$. The analysis consists in deriving from M_0 all possible markings (e.g. Fig. 8b) and checking that for each marking: (1) there is always at least one transition that can fire, i.e. PN has no deadlock; (2) number of tokens in each place is either 0 or 1, i.e. PN is safe; and (3) total number of tokens in any marking is same (strictly conservative) or variable (partially conservative).

Place/transition invariants analysis: Place invariants are used to study two properties: 1) network safety, and 2) network conservativeness. Transition invariants show the lack of deadlocks in the network. Safety analysis requires solving Eq. (4). If all places of the network belong to $\|\mathbf{y}\|$ and M_0 is bounded (i.e., the sum of tokens in M_0 is finite) then the network is bounded. If for each $\|\mathbf{y}\|$ the sum of tokens is 1 then the network is safe.

Conservatism analysis also employs solutions of Eq. (4). The vector of weights can be obtained just by summing all the linearly independent vectors that are place invariants. If the resulting vector is $(1, \dots, 1)^T$, then the network is strictly conservative. If no place invariant is found for the network except $\mathbf{y} = \mathbf{0}$, then the network is not conservative. On the other hand, if some component of the vector is 0 (but $\mathbf{y} \neq \mathbf{0}$) then the network is partially conservative. In other cases, the network is conservative.

A network is free of deadlocks if it is live [21]. A network is considered live if, for every reachable marking M_m , there exists a sequence of transition firings in which each transition can potentially fire at least once. If, based on $N^T \cdot \mathbf{x} = \mathbf{0}$, we can find a vector \mathbf{x} that is a transition invariant with non-zero values for each transition, then firing all transitions indicated in \mathbf{x} from any reachable marking M_m will return the marking to M_m . According to [21], this confirms that the network is live. Thus, if every transition can potentially fire from each reachable marking M_m , there are no deadlocks in the network.

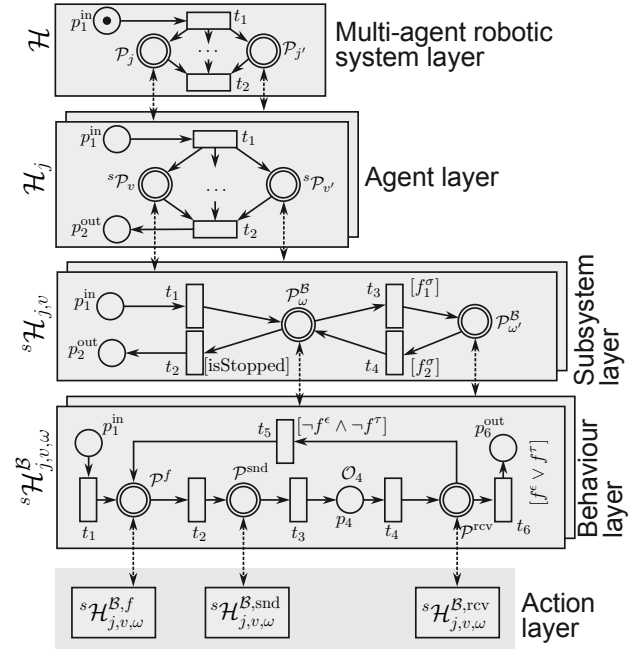


Fig. 2: RSHPN \mathcal{H} modeling activities of a robotic system

F. Justification of conservativeness analysis

The structure of \mathcal{H} assures that when any subnet is activated, a single token appears in its input place. Since each network in \mathcal{H} is meant to be safe, the parent PN cannot introduce another token to an already activated subnet. The number of tokens in an activated subnet changes only by firing its transitions. Hence, a subnet is conservative and to what extent depends on its structure, not on the parent network. In effect the parent PN can be treated as a transition connecting the output place to the input place of the analysed subnet. Hence, in a strictly conservative PN at any time the number of tokens is always constant and exactly one, i.e. subnet will always execute exactly one operation at any time (as it has a single token in an input place in the initial marking M_0). Ultimately, each subnet in an RSHPN ends up with exactly one token in its output place. Changes in PN marking can be examined through conservativeness analysis.

IV. ROBOTIC SYSTEM HIERARCHICAL PETRI NET

RSHPN \mathcal{H} is a HPN adopted to model the activity of the whole multi-agent robotic system \mathcal{RS} . It consists of six layers (Fig. 2). RSHPN decomposition into layers reflects the structure of \mathcal{RS} [15]. Each RSHPN layer describes system activities at a different level of abstraction: 1) system composed of agents, 2) agent structure, 3) task definition for subsystems, 4) behaviour definition for each subsystem (a pattern parameterised by a transition function), 5) decomposition of a transition function and communication model definition, 6) general parameterised model of communication. This defines the robotic system's structure and the activity of its components. The initial marking is in Fig. 2. A single token enters at the top and propagates through lower layers, multiplying appropriately as it moves.

A. Description of RSHPN layers

Multi-agent robotic system layer: contains a single net \mathcal{H} (Fig. 2) representing the \mathcal{RS} task \mathcal{T} aggregating tasks executed by all agents (activities of a_j are represented by \mathcal{P}_j). At system initiation t_1 fires, activating in parallel all pages for \mathcal{RS} agents. Once all pages complete their activities, t_2 fires and the system terminates its activities.

Agent layer: defines a single \mathcal{H}_j for each a_j . \mathcal{H}_j represents its task \mathcal{T}_j aggregating the tasks of its subsystems. \mathcal{H}_j contains a page ${}^s\mathcal{P}_{j,v}$ for each $s_{j,v}$ in a_j [15], [16]. All pages activate in parallel, allowing subsystems to act independently.

Subsystem layer: defines for each $s_{j,v}$ a single net ${}^s\mathcal{H}_{j,v}$ representing the task ${}^s\mathcal{T}_{j,v}$. The task determines how $s_{j,v}$ switches between its behaviours ${}^s\mathcal{B}_{j,v,\omega}$. Each ${}^s\mathcal{B}_{j,v,\omega}$ is represented by a page ${}^s\mathcal{P}_{j,v,\omega}^B$. For each pair of consecutive behaviors (e.g. ${}^s\mathcal{B}_{j,v,\omega}$ – current, and ${}^s\mathcal{B}_{j,v,\omega'}$ – next behaviour), there is a transition ${}^st_{j,v,\alpha}$ with initial condition ${}^sf_{j,v,\alpha}^\sigma$. When ${}^s\mathcal{B}_{j,v,\omega}$ terminates and ${}^sf_{j,v,\alpha}^\sigma$ is true, it switches to ${}^s\mathcal{B}_{j,v,\omega'}$. A single condition associated with transitions ${}^st_{j,v,\alpha}$ from ${}^s\mathcal{P}_{j,v,\omega}^B$ must be true at termination of ${}^s\mathcal{B}_{j,v,\omega}$. Condition [isStopped] is true if $s_{j,v}$ terminates.

Behaviour layer: defines for each behaviour ${}^s\mathcal{B}_{j,v,\omega}$ a single fixed-structure net ${}^s\mathcal{H}_{j,v,\omega}^B$ composed of pages for an elementary action ${}^s\mathcal{A}_{j,v,\omega}$, with terminal ${}^sf_{j,v,\omega}^\tau$ and error ${}^sf_{j,v,\omega}^e$ conditions. ${}^s\mathcal{A}_{j,v,\omega}$ consists of 3 pages and one operation, all executed unconditionally: 1) ${}^s\mathcal{P}_{j,v,\omega}^{B,f}$ calculates the transition function ${}^sf_{j,v,\omega}$, 2) ${}^s\mathcal{P}_{j,v,\omega}^{B,send}$ sends out the results of ${}^sf_{j,v,\omega}$ evaluation, 3) increments the discrete time stamp ι (operation ${}^s\mathcal{O}_{j,v,\omega}^B$), 4) ${}^s\mathcal{P}_{j,v,\omega}^{B,rcv}$ inserts the received data into $x^{s_{j,v}}$. If neither ${}^sf_{j,v,\omega}^e$ nor terminal ${}^sf_{j,v,\omega}^\tau$ are satisfied, ${}^st_{j,v,\omega,5}$ fires leading to the next iteration of ${}^s\mathcal{B}_{j,v,\omega}$. Otherwise, ${}^st_{j,v,\omega,6}$ fires, terminating ${}^s\mathcal{B}_{j,v,\omega}$, i.e. a single token appears in ${}^sp_{j,v,\omega,6}^B$ and the control returns to ${}^s\mathcal{H}_{j,v}$ which designates a new behaviour based on ${}^s\mathcal{T}_{j,v}$.

Action layer: defines 3 modules each divided into 2 layers for each behaviour ${}^s\mathcal{B}_{j,v,\omega}$: 1) ${}^s\mathcal{H}_{j,v,\omega}^{B,f}$ – defines transition function ${}^sf_{j,v,\omega}$ executed by $s_{j,v}$ realising ${}^s\mathcal{B}_{j,v,\omega}$, 2) ${}^s\mathcal{H}_{j,v,\omega}^{B,send}$ represents the send communication mode used by $s_{j,v}$, 3) ${}^s\mathcal{H}_{j,v,\omega}^{B,rcv}$ represents the receive communication mode used by $s_{j,v}$. For a more detailed description see [15].

B. Communication models

Subsystem $s_{j,v}$ communication modes are defined by two nets: a) ${}^s\mathcal{H}_{j,v,\omega}^{B,send}$ and b) ${}^s\mathcal{H}_{j,v,\omega}^{B,rcv}$. Each determines the order in which the $s_{j,v}$ communicates with its associated subsystems (the arrangement of pages). For each communicating pair of subsystems an inter-subsystem communication model is produced from these modes (Table III). Since each subsystem can communicate in three modes: blocking, blocking with timeout or non-blocking, nine possible inter-subsystem communication models result. All are realised by the PN presented in Fig. 3.

C. Complexity of RSHPN layers

RSHPN \mathcal{H} consists of four network types:

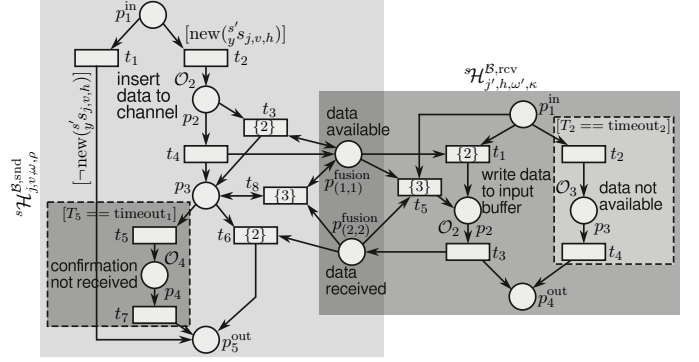


Fig. 3: General communication model for subsystems: $s_{j,v}$ (sender) and $s_{j,h}$ (receiver); 9 possible models.

TABLE III: Nine communication models realised by the PN in Fig. 3 depending on t_{out1} and t_{out2} , where ($t_{out\gamma} \triangleq \text{timeout}_\gamma, \gamma = 1, 2$); modes: NB – non-blocking, B – blocking, and BT – blocking with timeout

Communication mode		Receive		
		$t_{out2} = 0$	$t_{out2} = \infty$	$0 < t_{out2} < \infty$
Send	$t_{out1} = 0$	NB-NB	NB-B	NB-BT
	$t_{out1} = \infty$	B-NB	B-B	B-BT
	$0 < t_{out1} < \infty$	BT-NB	BT-B	BT-BT

- 1) trivial, variable structure: \mathcal{H} , \mathcal{H}_j , and assuming sequential or parallel arrangement: a) ${}^s\mathcal{H}_{j,v,\omega}^{B,f}$, b) ${}^s\mathcal{H}_{j,v,\omega}^{B,send}$ and c) ${}^s\mathcal{H}_{j,v,\omega}^{B,rcv}$, and ${}^s\mathcal{H}_{j,v,\omega}^{B,f}$,
- 2) trivial, fixed structure: ${}^s\mathcal{H}_{j,v,\omega}^B$,
- 3) complex, fixed structure: a network composed of ${}^s\mathcal{H}_{j,v,\omega}^{B,send}$ and ${}^s\mathcal{H}_{j,v,\omega}^{B,rcv}$ representing the general communication model for a pair of subsystems,
- 4) complex, variable structure: ${}^s\mathcal{H}_{j,v}$, and in hybrid arrangements: ${}^s\mathcal{H}_{j,v,\omega}^{B,f}$, ${}^s\mathcal{H}_{j,v,\omega}^{B,send}$, ${}^s\mathcal{H}_{j,v,\omega}^{B,rcv}$.

PN structure complexity affects the choice of analysis method: for simple PNs, use PN interpretation and reachability graphs, while for complex PNs, use place and transition invariants.

V. RSHPN META-MODEL ANALYSIS

PNs in RSHPN layers are analysed from the top layer to lower layers, as shown in the video tutorial³.

A. Multi-agent robotic system layer analysis

\mathcal{H} is composed of one PN. Its simplified structure is shown in Fig. 4. Assuming that lower-level PNs are correct the simplified PN is as in Fig. 5. By inspection we conclude that \mathcal{H} is safe (in every reachable marking, i.e. M_0 and M_1 , each place has at the most a single token), conservative (due to the vector of weights $\mathbf{y} = (|\hat{a}|, 1, \dots, 1)^\top$) and deadlock-free as in M_0 and M_1 , always a single transition can fire.

B. Agent layer analysis

The agent layer consists of $|\hat{a}|$ different \mathcal{H}_j . Each \mathcal{H}_j consists of a single input and single output place. Thus, the structure of \mathcal{H}_j can be extended with an additional transition.

³Introduction to the RSHPN analysis: <https://youtu.be/JenAB1IKVVY>

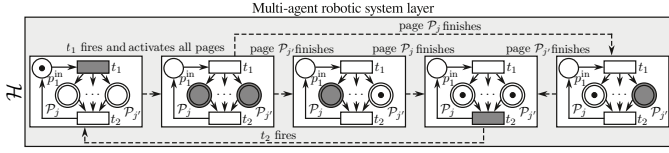


Fig. 4: Graphical analysis of \mathcal{H} (first layer of RSHPN in Fig. 2)

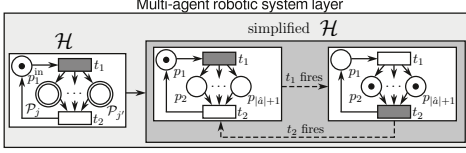


Fig. 5: Simplified \mathcal{H} has two markings: $M_0 = (1, 0, \dots, 0)^\top$ and $M_1 = (0, 1, \dots, 1)^\top$; $|\hat{a}|$ - number of agents in \mathcal{RS}

Assuming that the properties of lower level Petri nets, i.e. $\mathcal{H}_{j,v}$, are fulfilled, then the extended \mathcal{H}_j can be further simplified by changing pages into places, as in Fig. 6. Thus, the analysis of \mathcal{H}_j boils down to the analysis of the simplified Petri net. The number of tokens in each place within each reachable marking (i.e. M_0, M_1, M_2) is limited to 1, so \mathcal{H}_j is safe. Since from any reachable marking there is always a single transition ready to fire, the \mathcal{H}_j is deadlock-free. A vector of weights $\mathbf{y} = (|\hat{s}_j|, 1, \dots, 1, |\hat{s}_j|)^\top$ ensures that in the simplified \mathcal{H}_j the weighted sum of tokens is equal to $|\hat{s}_j|$, which means that \mathcal{H}_j is conservative.

C. Subsystem layer analysis

Subsystem layer contains $\sum_{a_j \in \hat{a}} |\hat{s}_j|$ panels, each holding a single PN ${}^s\mathcal{H}_{j,v}$. Analysis of ${}^s\mathcal{H}_{j,v}$ requires substitution of \mathcal{H}_j by a transition connecting ${}^s\mathcal{H}_{j,v}$ output with input place. Since ${}^s\mathcal{H}_{j,v}$ represents an arbitrary task ${}^s\mathcal{T}_{j,v}$ it assumes diverse structures. Hence, the analysis of ${}^s\mathcal{H}_{j,v}$ is based on an incidence matrix. A valid structure of ${}^s\mathcal{H}_{j,v}$ requires no self-loops and that within each row of incidence matrix ${}^sN_{j,v}$ exactly two non-zero numbers exist: -1 and 1 . If the assumptions are violated the PN structure is incorrect. E.g. for the PN in Fig. 7 the incidence matrix ${}^sN_{j,v}$ is as in Eq. (5).

$${}^sN_{j,v} = \begin{pmatrix} p_1^{in} & {}^s\mathcal{P}_{j,v,\omega'}^B & {}^s\mathcal{P}_{j,v,\omega''}^B & {}^s\mathcal{P}_{j,v,\omega'''}^B & p_5^{out} \\ -1 & 1 & 0 & 0 & 0 \\ 0 & -1 & 0 & 0 & 1 \\ 0 & 0 & 1 & 0 & 0 \\ 0 & 1 & -1 & 0 & 0 \\ 0 & -1 & 0 & 1 & 0 \\ 0 & 1 & 0 & -1 & 0 \\ 0 & 0 & -1 & 1 & 0 \\ 1 & 0 & 0 & 0 & -1 \end{pmatrix} \begin{matrix} t_1 \\ t_2 \\ t_3 \\ t_4 \\ t_5 \\ t_6 \\ t_7 \\ t_8 \end{matrix} \quad (5)$$

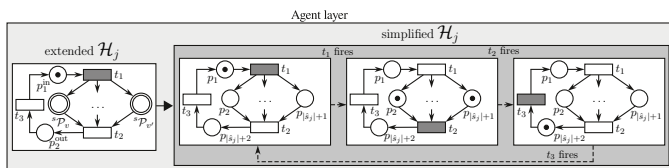


Fig. 6: Simplified \mathcal{H}_j ; $|\hat{s}_j|$ - number of subsystems in a_j ; $M_0 = (1, 0, \dots, 0, 0)^\top$, $M_1 = (0, 1, \dots, 1, 0)^\top$, $M_2 = (0, 0, \dots, 0, 1)^\top$

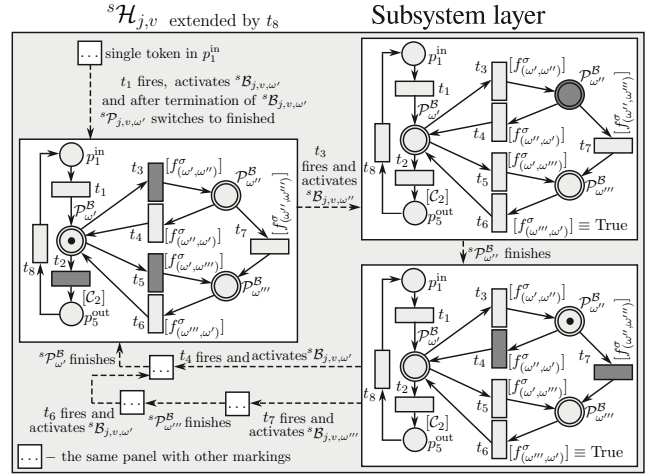


Fig. 7: Analysis of an exemplary ${}^s\mathcal{H}_{j,v}$

Satisfaction of the above requirements ensures strict conservativeness. To show the invariability of the token number in any M_m , it suffices to notice that when a transition fires, one token from a place/page is consumed, and one token is inserted into another place/page, hence $\mathbf{y} = (1, \dots, 1)^\top$.

To avoid deadlock, in any M_m exactly one transition should be able to fire, i.e. the condition associated with the transition must be met. To ensure deterministic execution of ${}^s\mathcal{H}_{j,v}$ conditions associated with transitions for which considered place/page is an input must satisfy: (1) the logical sum of all initial conditions must be True; and (2) the logical product of any two conditions must be False (e.g. if a token is in ${}^s\mathcal{P}_{j,v,\omega'}^B$ (Fig. 7), then: $[{}^s f_{(\omega',\omega'')}^\sigma \vee {}^s f_{(\omega',\omega''')}^\sigma \vee C_2] = \text{True}$, and $[({}^s f_{(\omega',\omega'')}^\sigma \wedge {}^s f_{(\omega',\omega''')}^\sigma = \text{False}) \wedge ({}^s f_{(\omega',\omega'')}^\sigma \wedge C_2 = \text{False}) \wedge ({}^s f_{(\omega',\omega''')}^\sigma \wedge C_2 = \text{False})] = \text{True}$). Both conditions must be met at the end of place/page activity. The first condition ensures at least one transition can fire, preventing deadlock in ${}^s\mathcal{H}_{j,v}$. The second condition ensures only one behaviour can be selected, ensuring determinism.

D. Behaviour layer analysis

The behaviour layer consists of $\sum_{a_j \in \hat{a}} \sum_{s_{j,v} \in \hat{s}_j} |{}^s\hat{\mathcal{B}}_{j,v}|$ panels. Each PN (panel) has exactly the same structure as ${}^s\mathcal{H}_{j,v}^B$ - this is the general behaviour ${}^s\mathcal{B}_{j,v,\omega}$ pattern (Fig.2). So instead of analysing all the PNs specified in all panels, it suffices to analyse a single PN being the pattern. Hence, PN in Fig. 8a is analysed only. In that network each transition has exactly one input place and exactly one output place, i.e. firing any transition does not change the number of tokens in the network. Thus, the network is strictly conservative. Since there is exactly one token in the initial marking, the network is safe. Moreover, for any reachable marking, there is always exactly one fireable transition (the conditions for the transitions t_5 and t_6 are mutually exclusive), thus there is no deadlock. Those properties can also be verified using the reachability graph presented in Table 8b. For each possible marking: a) each place has at the most a single token, i.e. PN is safe, b) total number of tokens remains always the same, i.e. the net is

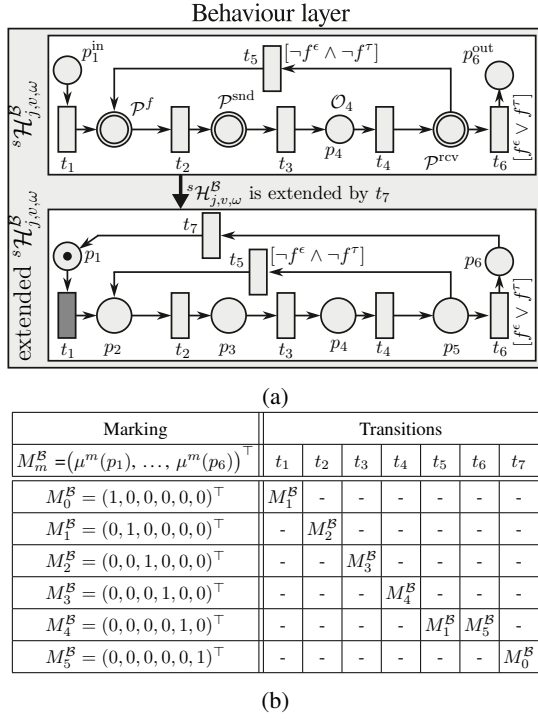


Fig. 8: (8a): extended $s\mathcal{H}_{j,v,\omega}^B$; (8b): tabular form of the reachability graph of extended $s\mathcal{H}_{j,v,\omega}^B$ (rows represent graph nodes, columns transitions (e.g. firing t_4 at M_3^B , leads to M_4^B))

strictly conservative, and c) for any reachable marking always a single transition can fire, i.e. net is deadlock-free.

E. Activity sublayers analysis

Analysis of the action layer requires the analysis of 3 PNs in $s\mathcal{H}_{j,v,\omega}^B$, namely: $s\mathcal{H}_{j,v,\omega}^{B,f}$, $s\mathcal{H}_{j,v,\omega}^{B, snd}$ and $s\mathcal{H}_{j,v,\omega}^{B, rcv}$. Each PN's structure depends on the organisation of $s f_{j,v,\omega}$ computations and communication, with pages activated: sequentially, in parallel or in a hybrid manner (defined by the user, potentially combining sequential and parallel structures). Typically PNs: $s\mathcal{H}_{j,v,\omega}^{B,f}$, $s\mathcal{H}_{j,v,\omega}^{B, snd}$ and $s\mathcal{H}_{j,v,\omega}^{B, rcv}$ adopt parallel arrangement since operation of pages can be independent, i.e. $s_{j,v}$ can independently send data from each output buffer. However, sending data sequentially can be preferable. For parallel arrangements, the analysis follows similar rules as for \mathcal{H}_j and for sequential arrangements, as the analysis of $s\mathcal{H}_{j,v,\omega}^B$. For hybrid configuration, defined by the developer, we follow rules similar to those used for $s\mathcal{H}_{j,v}$.

F. Analysis of the general communication model

PNs forming send and receive mode sublayers can not be analysed independently, as the last sublayer models the interaction between a pair of communicating subsystems where the PNs are connected by fusion places [15]. Both nets form a single PN representing the communication model for a pair of subsystems. Sec. IV-B introduces 9 different communication models, however, all of them can be represented by a single PN (Fig. 3). Thus a single PN is analysed. To produce its incidence matrix from the network in Fig. 3 three self-loops must be

removed: 1) $t_3 \leftrightarrow p_{(1,1)}^{fusion}$, 2) $t_8 \leftrightarrow p_3$, and 3) $t_8 \leftrightarrow p_{(1,1)}^{fusion}$. The result is a pure PN, i.e. without self-loops, (Fig. 9). This network is transformed into incidence matrix N^{model} (Eq. (6)) without losing information about the network operation.

$$N^{model} = \begin{pmatrix} p_1 & p_2 & p_3 & p_4 & p_5 & p_6 & p_7 & p_8 & p_9 & p_{10} & p_{11} & p_{12} & p_{13} \\ \begin{pmatrix} -1 & 0 & 0 & 0 & 1 & 0 & 0 & 0 & 0 & 0 & 0 & 0 & 0 \\ -1 & 1 & 0 & 0 & 0 & 0 & 0 & 0 & 0 & 0 & 0 & 0 & 0 \\ 0 & -1 & 0 & 0 & 0 & -1 & 0 & 0 & 0 & 0 & 0 & 1 & 0 \\ 0 & 0 & -1 & 0 & 0 & 1 & 0 & 0 & 0 & 0 & 0 & 0 & 0 \\ 0 & 0 & -1 & 1 & 0 & 0 & 0 & 0 & 0 & 0 & 0 & 0 & 0 \\ 0 & 0 & -1 & 0 & 1 & 0 & -1 & 0 & 0 & 0 & 0 & 0 & 0 \\ 1 & 0 & 0 & 0 & -1 & 0 & 0 & 0 & 0 & 0 & 0 & 0 & 0 \\ 0 & 0 & 0 & 0 & 0 & 0 & 0 & -1 & 1 & 0 & 0 & 0 & 0 \\ 0 & 0 & 0 & 0 & 0 & 0 & 0 & 0 & 1 & 0 & 0 & 0 & 0 \\ 0 & 0 & 0 & 0 & 0 & 0 & 0 & -1 & -1 & -1 & 1 & 0 & 0 \\ 0 & 0 & 0 & 0 & 0 & 0 & 0 & 0 & 0 & 0 & 1 & 0 & 0 \\ 0 & 0 & 1 & 0 & 0 & 1 & 0 & 0 & 0 & 0 & 0 & -1 & 0 \\ 0 & 0 & 0 & 1 & 0 & 0 & 0 & 0 & 0 & 0 & 0 & 0 & -1 \\ 0 & 0 & 0 & 0 & 0 & 0 & 0 & 0 & 0 & 0 & 0 & 0 & 0 \end{pmatrix} & \begin{pmatrix} t_1 \\ t_2 \\ t_3 \\ t_4 \\ t_5 \\ t_6 \\ t_7 \\ t_8 \\ t_9 \\ t_{10} \\ t_{11} \\ t_{12} \\ t_{13} \\ t_{14} \\ t_{15} \\ t_{16} \\ t_{17} \end{pmatrix} \end{pmatrix} \quad (6)$$

Eq. (7) (transition invariant) and Eq. (8) (place invariant) are solved assuming: $\mathbf{x}^{model} \neq \mathbf{0}$, $\mathbf{y}^{model} \neq \mathbf{0}$ and restricting the solution to non-negative integers.

$$(N^{model})^T \cdot \mathbf{x}^{model} = (0, 0, 0, 0, 0, 0, 0, 0, 0, 0, 0, 0, 0)^T \quad (7)$$

$$N^{model} \cdot \mathbf{y}^{model} = (0, 0, 0, 0, 0, 0, 0, 0, 0, 0, 0, 0, 0, 0, 0, 0)^T \quad (8)$$

For $x_\delta \in \{x_9, x_{12}, x_{14}, x_{15}, x_{16}, x_{17}\}$, assuming that $x_\delta \in \mathbb{Z}$ and $x_\delta > 0$, Eq. (9) is produced, thus determining the transition invariants.

$$\mathbf{x}^{model} = \begin{pmatrix} x_9 + x_{14} - x_{15} - x_{16} \\ -x_{14} + x_{15} + x_{16} \\ x_{16} \\ -x_{14} + x_{15} \\ x_{17} \\ x_{12} + x_{16} + x_{17} \\ -x_{12} - x_{14} + x_{15} - x_{17} \\ x_{12} + x_{16} + x_{17} \\ x_9 \\ -x_{12} - x_{14} + x_{15} \\ x_{14} \\ x_{12} \\ -x_{14} + x_{15} \\ x_{14} \\ x_{15} \\ x_{16} \\ x_{17} \end{pmatrix} \quad (9) \quad \mathbf{y}^{model} = \begin{pmatrix} y_{13} \\ y_{13} \\ y_{13} \\ y_{13} \\ y_{13} \\ 0 \\ 0 \\ y_{11} \\ y_{11} \\ y_{11} \\ y_{11} \\ y_{13} \\ y_{13} \end{pmatrix} \quad (10)$$

Now the positive transition invariant is determined, for which $\|\mathbf{x}^{model}\|$ contains the maximum number of different transitions. Setting $x_9 = 5$, $x_{12} = 1$, $x_{14} = 1$, $x_{15} = 4$, $x_{16} = 1$, $x_{17} = 1$, then $\mathbf{x}^{model} = (1, 4, 1, 3, 1, 3, 1, 3, 5, 2, 1, 1, 3, 1, 4, 1, 1)^T$. Thus firing all the transitions as many times as \mathbf{x}^{model} indicates, the network will return to M_0 . As shown in Sec. III-E, if it is possible to reach M_0 by firing all transitions in the PN then the net is live. And since it is live there are no deadlocks. Interestingly, by manipulating the parameters x_9 , x_{12} , x_{14} , x_{15} , x_{16} and x_{17} one can obtain different combinations of sender and receiver modes, e.g.:

- if $x_9 = 1$ (all others equal zero) then $\mathbf{x}^{model} = (1, 0, 0, 0, 0, 0, 0, 0, 1, 0, 0, 0, 0, 0, 0, 0, 0)$. The vector obtained indicates that the sending subsystem does not compute new data and therefore does not send any data. After firing t_1 and t_9 , the network marking returns to the initial M_0 marking, i.e. $M_0 \xrightarrow{t_1} \dots \xrightarrow{t_9} M_0$,

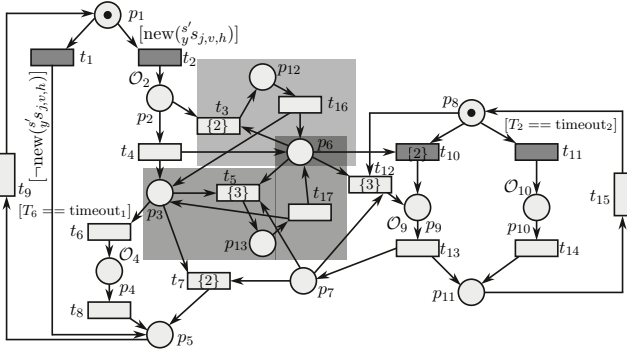


Fig. 9: Pure Petri net (communication model from Fig. 3)

- if $x_9 = 1, x_{15} = 1, x_{17} = 1$ then $\mathbf{x}^{\text{model}} = (0, 1, 0, 1, 1, 0, 1, 0, 1, 1, 0, 0, 1, 0, 1, 0, 1)$. If the transitions indicated in the vector fire, e.g. in the order: $t_2 \rightarrow t_4 \rightarrow t_{10} \rightarrow t_{13} \rightarrow t_5 \rightarrow t_{17} \rightarrow t_7 \rightarrow t_9 \rightarrow t_{15}$, then successful communication will take place between the sender and receiver (both operating in blocking mode),
- if $x_9 = 2, x_{14} = 1, x_{15} = 2, x_{16} = 1, x_{17} = 1$ then $\mathbf{x}^{\text{model}} = (0, 2, 1, 1, 1, 2, 0, 2, 2, 1, 1, 0, 1, 1, 2, 1, 1)$. If the transitions indicated in the vector fire, e.g. in the order: $t_2 \rightarrow t_4 \rightarrow t_6 \rightarrow t_8 \rightarrow t_9 \rightarrow t_2 \rightarrow t_3 \rightarrow t_{16} \rightarrow t_{10} \rightarrow t_{13} \rightarrow t_{15} \rightarrow t_5 \rightarrow t_{17} \rightarrow t_6 \rightarrow t_8 \rightarrow t_9 \rightarrow t_{11} \rightarrow t_{14} \rightarrow t_{15}$ then communication will take place between the two subsystems operating in non-blocking mode.

Eq. (10), where: $y_{11}, y_{13} \in \mathbb{Z}$ and $y_{11}, y_{13} > 0$, represents the solution of Eq. (8). The vector $\mathbf{y}^{\text{model}}$ determines all possible place invariants. Two linearly independent place invariants can be derived: a) ${}^1\mathbf{y}^{\text{model}} = (1, 1, 1, 1, 1, 0, 0, 0, 0, 0, 0, 1, 1)^T$ for $y_{13} = 1 \wedge y_{11} = 0$, and b) ${}^2\mathbf{y}^{\text{model}} = (0, 0, 0, 0, 0, 0, 0, 0, 1, 1, 1, 1, 0, 0)^T$ for $y_{13} = 0 \wedge y_{11} = 1$, thus the weighted sum of the tokens remains constant for each reachable marking M_m , i.e.: $M_m^T \cdot {}^1\mathbf{y}^{\text{model}} = M_0^T \cdot {}^1\mathbf{y}^{\text{model}} = 1$ and $M_m^T \cdot {}^2\mathbf{y}^{\text{model}} = M_0^T \cdot {}^2\mathbf{y}^{\text{model}} = 1$, where $M_0 = (1, 0, 0, 0, 0, 0, 0, 0, 1, 0, 0, 0, 0, 0)^T$. From the above two equations, Eq. (11) and Eq. (12) are derived, which are satisfied for any reachable M_m .

$$M_m(p_1) + \dots + M_m(p_5) + M_m(p_{12}) + M_m(p_{13}) = 1 \quad (11)$$

$$M_m(p_8) + M_m(p_9) + M_m(p_{10}) + M_m(p_{11}) = 1 \quad (12)$$

It follows from Eq. (11) that the sum of the tokens in $p_1, p_2, p_3, p_4, p_5, p_{12}$ and p_{13} always equals 1, similarly, for p_8, p_9, p_{10}, p_{11} based on Eq. (12). Then, to prove that the PN (Fig. 9) is safe, it suffices to show that for any marking M_m : $M_m(p_6) \leq 1$, and $M_m(p_7) \leq 1$ (since the condition for the remaining places is satisfied, as follows from Eq. (11) and Eq. (12)). To prove the first one, a single token inserted into p_6 by either t_{16} (requires prior firing of t_3) or t_4 . The choice which transition fires, when $M_m(p_2) = 1$, depends on the current marking of p_6 . If $M_m(p_6) = 0$ then t_4 fires producing a single token in p_6 , i.e. as a result $M_m(p_6) = 1$. Otherwise, if $M_m(p_6) = 1$ then t_3 fires consuming a token from p_6 and produces a token in p_{12} . Subsequently, t_{16} fires producing a token in p_6 . As a result the number of tokens in p_6 remains the same. Thus, tokens will never multiply in

p_6 and $M_m(p_6) \leq 1$. Similar inference is made for p_7 based on t_{12} and t_{13} . Transitions t_3 and t_{12} assure that the tokens do not multiply within p_6 and p_7 , respectively (if the token was not consumed by t_{10} and t_7). Summarizing, for each p_i ($i = 1, \dots, 13$) and any marking M_m , the $M_m(p_i) \leq 1$ is always fulfilled, thus the PN is safe.

The obtained place invariants are used to check whether the PN is conservative. It is sufficient to sum the two obtained minimal place invariants, i.e. ${}^1\mathbf{y}^{\text{model}}$ and ${}^2\mathbf{y}^{\text{model}}$. This yields a vector of non-negative weights $(1, 1, 1, 1, 1, 0, 0, 1, 1, 1, 1, 1, 1)^T$, for which the weighted number of tokens in any reachable marking is equal to 2. Thus the PN is partially conservative. Moreover, it can be demonstrated that the PN can perform two operations simultaneously, i.e. sending from ${}_y s_{j,v}$ and receiving into ${}_x s_{j',h}$.

VI. KEY ANALYSIS OBSERVATIONS

Properties preservation: RSHPN meta-model analysis confirms \mathcal{H} is safe and conservative. Table IV summarizes meta-model properties preservation for each layer. The first column names the layer; the second indicates if the net is user-defined ('yes') or derived from the meta-model ('no') – where 'yes' requires full PN analysis and 'no' preserves meta-model properties. The third column shows conservativeness preservation, the fourth lists the vector of weights \mathbf{y} , and the fifth gives the weighted sum of tokens. In \mathcal{H} , subnets include: (1) strictly conservative – performing one operation at a time, (2) conservative – performing multiple operations simultaneously, or (3) partially conservative – performing exactly two operations. If a PN fails to produce the correct weighted sum, it is incompatible with the meta-model and must be corrected. This enables the automation of RSHPN analysis. Table IV indicates that RSHPN model analysis focuses on networks with a task-dependent (variable) structure (layers with 'yes'): 1) produced by the designer, i.e. those in subsystem layer or having hybrid arrangement, and 2) modeling the interaction between communicating subsystems (only if B-B mode is used). This property of RSHPN significantly reduces the analysis effort. If all subsystems of \mathcal{RS} communicate in non-blocking mode, and all operations performed by the subsystems are either sequential or parallel, the analysis of the developed \mathcal{H} model further reduces to the analysis of the networks in the subsystem layer only. Properties of PNs in other layers are preserved from the meta-model since these PNs have the same structure.

State space explosion: Assuming each agent has the same number of subsystems and each subsystem has the same number of behaviours, input and output buffers, the number of places in \mathcal{H} is approximated by:

$$\text{places}(\mathcal{H})^{\text{simple}} = |\hat{a}|(|\hat{s}_j| \cdot |{}^s \hat{\mathcal{B}}_{j,v}| \cdot (2^{|x \hat{s}_j, v}| \cdot (|y \hat{s}_j, v| + 1) + 7 \cdot |x \hat{s}_j, v| + 11 \cdot |y \hat{s}_j, v| + 16) + 3 \cdot |\hat{s}_j|) + 3 \cdot |\hat{a}| + 1$$

where: \hat{a} , \hat{s}_j , ${}^s \hat{\mathcal{B}}_{j,v}$, ${}_x \hat{s}_j, v$, ${}_y \hat{s}_j, v$ are sets of: agents, subsystems in each agent a_j , behaviours in $s_{j,v}$ and input and output buffers, respectively. For \mathcal{RS} with $|\hat{s}_j|$ subsystems operating

TABLE IV: Summary of RSHPN \mathcal{H} analysis regarding conservativeness (where $\zeta = |y\hat{s}_{j,v}|$, $\nu = |x\hat{s}_{j,v}|$)

Petri net	User defined	Conservative	Vector \mathbf{y}	Weighted sum
\mathcal{H}	no	yes	$(\hat{a} , 1, \dots, 1)$	$ \hat{a} $
\mathcal{H}_j	no	yes	$(\hat{s}_j , 1, \dots, 1, \hat{s}_j)$	$ \hat{s}_j $
${}^s\mathcal{H}_{j,v}$	yes	strictly	$(1, \dots, 1)$	1
${}^s\mathcal{H}_{j,v,\omega}^B$	no	strictly	$(1, \dots, 1)$	1
${}^s\mathcal{H}_{j,v,\omega,\psi}^B, {}^s\mathcal{H}_{j,v,\omega,\rho}^B, {}^s\mathcal{H}_{j,v,\omega,\kappa}^B$	no	strictly	$(1, \dots, 1)$	1
sequential	no	strictly	$(1, \dots, 1)$	1
parallel	no	yes	$(\zeta, 1, \dots, 1, \zeta)$	ν
hybrid	yes	yes	depends on the structure	
${}^s\mathcal{H}_{j,v,\omega,\psi}^B, {}^s\mathcal{H}_{j,v,\omega,\rho}^B, {}^s\mathcal{H}_{j,v,\omega,\kappa}^B$	no	strictly	$(1, \dots, 1)$	1
${}^s\mathcal{H}_{j,v,\omega,\rho}^B, {}^s\mathcal{H}_{j,v,\omega,\kappa}^B$	no	partially	$(1, 1, 1, 1, 1)$	2
${}^s\mathcal{H}_{j,v,\omega,\kappa}^B$	no	partially	$(0, 0, 1, 1, 1, 1)$	

in parallel for each $a_j \in \hat{a}$, the estimated number of states in the reachability graph depends on the exponent $|\hat{s}_j| \cdot |\hat{a}|$:

$$\text{states_in_reachability_graph}(\mathcal{H}) = [{}^s\hat{\mathcal{B}}_{j,v}] \cdot (2^{|x\hat{s}_{j,v}|} \cdot (|y\hat{s}_{j,v}| + 1) + 7 \cdot |x\hat{s}_{j,v}| + 11 \cdot |y\hat{s}_{j,v}| + 16) + 3 \cdot |\hat{s}_j|^{|\hat{s}_j| \cdot |\hat{a}|}$$

This leads to an exponential increase in the number of possible states in the reachability graph, making it infeasible to analyze even for relatively simple systems using standard methods. An example of table tennis balls collecting robot illustrates this [15]. In this article, we propose decomposing RSHPN analysis into the analysis of individual Petri nets in panels. As the number of panels depends on agents, subsystems, and behaviors (e.g., the estimated number of panels in the first four layers is $1 + |\hat{a}| + |\hat{a}| \cdot |\hat{s}_j| + |\hat{a}| \cdot |\hat{s}_j| \cdot |\hat{\mathcal{B}}_{j,v}|$), the number of necessary states in the reachability graphs no longer depends on the exponent $|\hat{s}_j| \cdot |\hat{a}|$. This key contribution ensures only user-dependent layers, such as the subsystem layer and those with hybrid arrangements, need the analysis, while others preserve the meta-model properties.

VII. CASE STUDY: SYSTEM ANALYSIS

A non-trivial robotic system for collecting table tennis balls [15] (from Fig. 12) was developed using the approach based on the RSHPN parametric meta-model. The system has a variable structure.

Task description: The main task of this robotic system is to collect table-tennis balls scattered on a flat surface. It is required that the robot operates in either of two modes: autonomous or teleoperated. The robot switches between them based on the recognised voice commands uttered by the operator, and terminates its operation when the termination command is issued. In the autonomous mode the robot, using its receptors and effectors, autonomously moves in the environment collecting table-tennis balls, while in the teleoperated mode the robot is controlled by operator commands.

System structure: The structure of the robotic system is presented in Fig. 10. It consists of 6 agents, out of which 4 are always active: 1) a_{audio} – responsible for sound synthesis and user voice command recognition, 2) a_{super} – supervisor agent responsible for task agent management and for transferring of recognised control commands, 3) $a_{\text{img_proc}}$ – responsible

for table-tennis ball detection based on neural networks, and 4) a_{bc} – controlling the robot hardware based on commands received from the task agents. Two other agents: a_{auto} (autonomous agent) and a_{tele} (teleoperated agent), are activated by a_{super} when the user issues voice-commands. The task agents are responsible for task execution. Only one of them can be active at a time.

RSHPN model: The activity of the whole robotic system, modeled using a single RSHPN \mathcal{H} , is presented in Fig. 11. The RSHPN has 1168 places and 1294 transitions, resulting in over 25 million reachable markings (states). Our previous approach to analysis, i.e. which was to flatten the PN and use state-of-the-art analysis tools (such as the Tina tool), proved to be inadequate. The results presented in this article show that for RSHPN it is possible to significantly reduce the complexity of the analysis.

Analysis: As shown in Table IV, the analysis of RSHPN is reduced to the analysis of PNs from the subsystem layer, PNs that form a communication model, and those that use a hybrid arrangement. However, since in the robotic system under analysis, the subsystems communicate with each other using non-blocking mode, and both the communication and transition functions are arranged in a sequential arrangement, the analysis of \mathcal{H} amounts to the analysis of PNs from the subsystem layer. Here only the analysis of two selected networks is presented, i.e. ${}^c\mathcal{H}_{\text{super,cs}}$ (Fig. 12) and ${}^c\mathcal{H}_{\text{auto,cs}}$ (Fig. 13), both extended accordingly. The remaining PNs are either trivial or relatively easy to analyse.

For the purpose of the analysis, the network ${}^c\mathcal{H}_{\text{auto,cs}}$ was extended to the form shown in Fig. 13. As shown in Fig. 13, each transition has exactly one input place and exactly one output place. This means that firing any transition does not change the number of tokens in the network, hence such Petri net is strictly conservative. Since in the activated network ${}^c\mathcal{H}_{\text{auto,cs}}$ the network $\mathcal{H}_{\text{auto}}$ cannot insert an additional token (otherwise the safety property for the network $\mathcal{H}_{\text{auto}}$ will not be fulfilled; remember that the whole \mathcal{H} was generated automatically following the RSHPN meta-model rules), this means that there is always exactly one token in the activated network ${}^c\mathcal{H}_{\text{auto,cs}}$ (the number of tokens is invariant, i.e. equals one). Thus the network is safe. In order to prove the absence of deadlock, it is necessary to look at both the network structure and the conditions associated with the transitions. It is enough to show that for each reachable marking (there

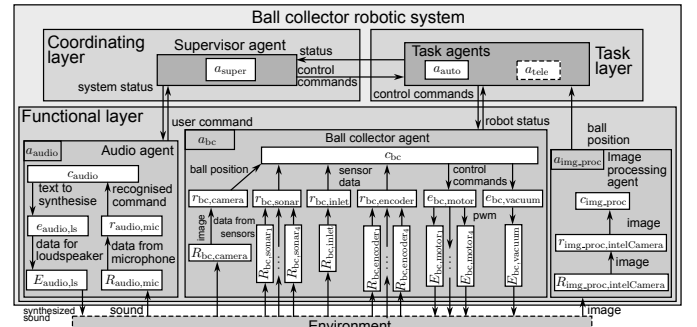


Fig. 10: Structure of the ball collector robotic system

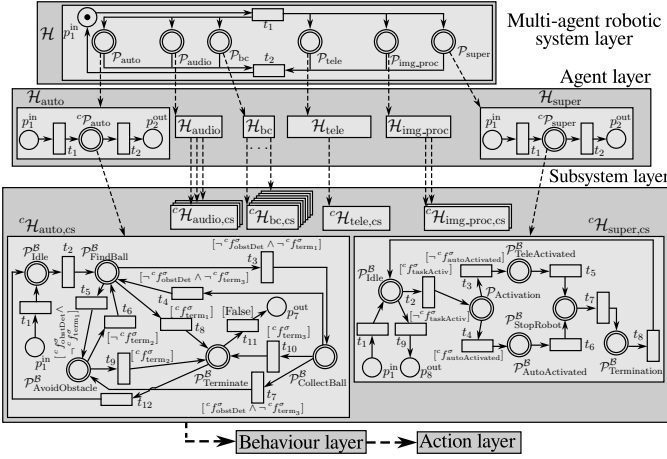


Fig. 11: RSHPN \mathcal{H} modelling the activity of the robotic system (Fig. 10)

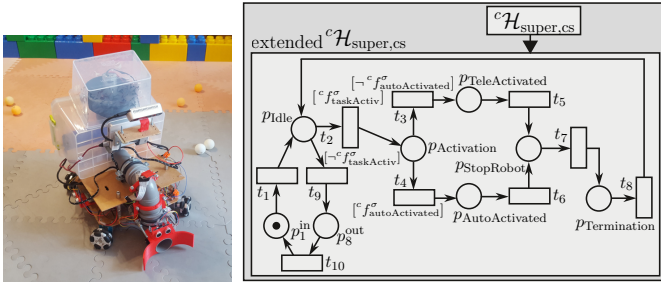


Fig. 12: Left: Robot collecting balls; right: extended $c^{\mathcal{H}}_{super,cs}$ modelling the activities of c_{super} .

are 7 markings because only a single token circulates among 7 places) there is always at least one transition ready to be fired (the assumption to be tested will be in fact more strict, namely whether there is exactly one transition ready to be fired). When a single token resides in one of the places: p_1^{in} , p_{Idle} , $p_{Terminante}$, and p_7^{out} it is clear, that always exactly one transition is fireable, namely, t_1 , t_2 , t_{12} , and t_{13} , respectively. $p_{FindBall}$ requires verification of the conditions associated with three transitions: t_3 ($\mathcal{C}_3 = [\neg^c f_{obsDet}^\sigma \wedge \neg^c f_{term1}^\sigma]$), t_5 ($\mathcal{C}_5 = [^c f_{obsDet}^\sigma \wedge \neg^c f_{term1}^\sigma]$) and t_8 ($\mathcal{C}_8 = [^c f_{term1}^\sigma]$). It suffices to show that when the token appears in $p_{FindBall}$ the following conditions are satisfied: 1) $[\mathcal{C}_3 \vee \mathcal{C}_5 \vee \mathcal{C}_8] = \text{True}$; 2) $\mathcal{C}_3 \wedge \mathcal{C}_5 = \text{False}$; 3) $\mathcal{C}_3 \wedge \mathcal{C}_8 = \text{False}$; and

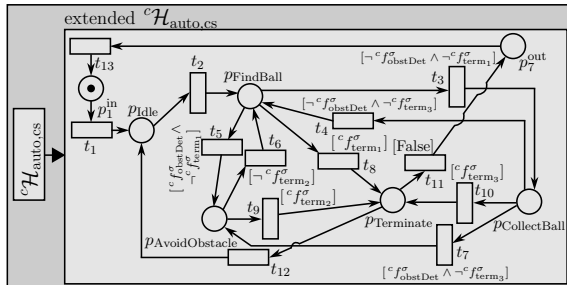


Fig. 13: Extended $c^{\mathcal{H}}_{auto,cs}$ modelling the activities of c_{auto} .

4) $\mathcal{C}_5 \wedge \mathcal{C}_8 = \text{False}$. The logical sum of the three conditions is always True since: $[\neg^c f_{obsDet}^\sigma \wedge \neg^c f_{term1}^\sigma] \vee [^c f_{obsDet}^\sigma \wedge \neg^c f_{term1}^\sigma] \vee [^c f_{term1}^\sigma] = [(\neg^c f_{obsDet}^\sigma \vee ^c f_{obsDet}^\sigma) \wedge \neg^c f_{term1}^\sigma] \vee [^c f_{term1}^\sigma] = [\neg^c f_{term1}^\sigma] \vee [^c f_{term1}^\sigma] = \text{True}$. On the other hand, logical products of consecutive condition pairs always produce False: 1) $\mathcal{C}_3 \wedge \mathcal{C}_5 = [\neg^c f_{obsDet}^\sigma \wedge \neg^c f_{term1}^\sigma] \wedge [^c f_{obsDet}^\sigma \wedge \neg^c f_{term1}^\sigma] = [\neg^c f_{term1}^\sigma \wedge (\neg^c f_{obsDet}^\sigma \wedge ^c f_{obsDet}^\sigma)] = \text{False}$, 2) $\mathcal{C}_3 \wedge \mathcal{C}_8 = [\neg^c f_{obsDet}^\sigma \wedge \neg^c f_{term1}^\sigma] \wedge [^c f_{term1}^\sigma] = \text{False}$ (since $\neg^c f_{term1}^\sigma \wedge ^c f_{term1}^\sigma = \text{False}$) and, 3) $\mathcal{C}_5 \wedge \mathcal{C}_8 = [^c f_{obsDet}^\sigma \wedge \neg^c f_{term1}^\sigma] \wedge [^c f_{term1}^\sigma] = \text{False}$ (since $\neg^c f_{term1}^\sigma \wedge ^c f_{term1}^\sigma = \text{False}$). An analogous analysis should be performed for the other two places, namely $p_{AvoidObstacle}$ and $p_{CollectBall}$. In the case where the token appears in $p_{AvoidObstacle}$ only one transition is ready to fire because the conditions associated with the transitions t_6 and t_9 , i.e. $\mathcal{C}_6 = [\neg^c f_{term2}^\sigma]$, and $\mathcal{C}_9 = [^c f_{term2}^\sigma]$, respectively, are mutually exclusive. On the other hand, three transitions are enabled when a token appears in $p_{CollectBall}$, namely: t_4 ($\mathcal{C}_4 = [\neg^c f_{obsDet}^\sigma \wedge \neg^c f_{term3}^\sigma]$), t_7 ($\mathcal{C}_7 = [^c f_{obsDet}^\sigma \wedge \neg^c f_{term3}^\sigma]$), and t_{10} ($\mathcal{C}_{10} = [^c f_{term3}^\sigma]$). Proving that: 1) $\mathcal{C}_4 \vee \mathcal{C}_7 \vee \mathcal{C}_{10}$, 2) $\mathcal{C}_4 \wedge \mathcal{C}_7$, 3) $\mathcal{C}_4 \wedge \mathcal{C}_{10}$ and 4) $\mathcal{C}_7 \wedge \mathcal{C}_{10}$, is straightforward enough to be omitted. This leads to the final conclusion that for each reachable marking in the extended $c^{\mathcal{H}}_{auto,cs}$ always at least a single transition is fireable, i.e. the $c^{\mathcal{H}}_{auto,cs}$ is deadlock-free.

The analysis of the extended $c^{\mathcal{H}}_{super,cs}$ (Fig. 12) should be carried out in a similar way. It can be seen that in the extended $c^{\mathcal{H}}_{super,cs}$ each transition has exactly one input place and exactly one output place. Consequently, the network is strictly conservative. Considering that and the fulfilment of the safety property by \mathcal{H}_{super} , in the extended $c^{\mathcal{H}}_{super,cs}$ there can be exactly one token. This leads to the conclusion that $c^{\mathcal{H}}_{super,cs}$ is safe. As there can be only one token circulating in $c^{\mathcal{H}}_{super,cs}$, the number of reachable markings equals to the number of places, i.e. 8. In the case where a single token resides in one of the six places, i.e. p_1^{in} , $p_{TeleActivated}$, $p_{AutoActivated}$, $p_{StopRobot}$, $p_{Termination}$, p_8^{out} , then exactly one transition is fireable (because each place has exactly one output transition, and each of output transitions has its condition set to the default value, i.e. True): t_1 , t_5 , t_6 , t_7 , t_8 and t_{10} , respectively. In the case of place p_{Idle} , the conditions associated with its output transitions: t_2 and t_9 , are mutually exclusive (since $\mathcal{C}_2 = [^c f_{taskActiv}^\sigma]$ and $\mathcal{C}_9 = [\neg^c f_{taskActiv}^\sigma]$). Similarly, in the case of place $p_{Activation}$, the conditions associated with its output transitions: t_3 and t_4 , are mutually exclusive (since $\mathcal{C}_3 = [\neg^c f_{autoActivated}^\sigma]$ and $\mathcal{C}_4 = [^c f_{autoActivated}^\sigma]$). This leads to the final conclusion that for each reachable marking of the extended $c^{\mathcal{H}}_{super,cs}$ there is always exactly one fireable transition. This proves that the network $c^{\mathcal{H}}_{super,cs}$ is deadlock-free.

Taking into account the above considerations, it can be concluded that the network \mathcal{H} is safe, deadlock-free and it satisfies the conservativeness assumptions presented in Table IV.

VIII. DISCUSSION

Selected methods for property verification: In this paper, we have selected three methods for analysing Petri Nets (PNs), focusing on their simplicity and applicability to specific

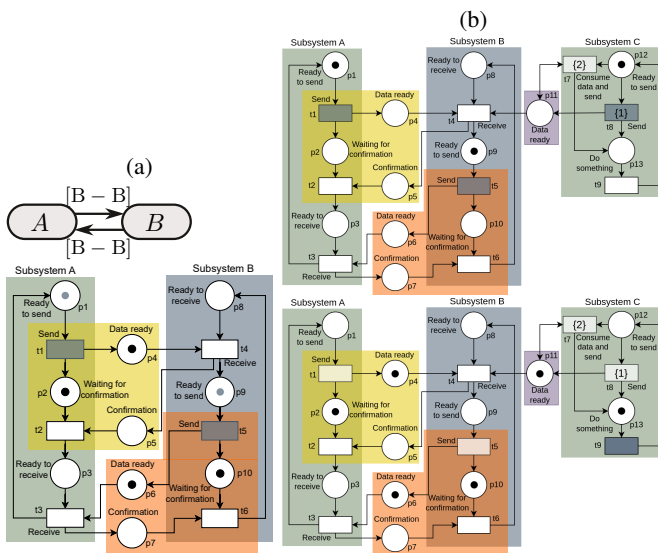


Fig. 14: **(a)**: Subsystems A and B send and receive data in blocking mode. If A starts with a token in p_1 and B in p_9 then the deadlock occurs. However, if they are appropriately initialised, i.e. A starts with p_1 and B with p_{10} then there is no deadlock; **(b)**: Example of a local deadlock, without global deadlock. Subsystem A and B have no transition to fire, while subsystem C has. Right top: initial marking, Right bottom: occurrence of local deadlock (after firing: t_1, t_5, t_8, t_9, t_7). The priority of t_7 ($\{2\}$) is higher than that of t_8 ($\{1\}$).

layers of the RSHPN model. These methods include graphical network state analysis (simulating the network), reachability graph analysis, and analysis based on place and transition invariants. They were chosen because they sufficiently verify key system properties such as safety, conservatism, and deadlock freedom. However, other methods, such as critical path analysis or temporal analysis, could also be used to explore additional properties. Future enhancements could include incorporating temporal analysis for tasks or communication models, and combining model checking with runtime verification by leveraging the meta-model checking approach.

Our primary goal was to develop a method to decompose the analysis into manageable parts. For each RSHPN layer, we specify the most appropriate analysis method and identify which layers do not require repeated analysis. For example, general patterns, such as the behavior or communication model layers, only need to be analyzed once. Networks generated by populating the RSHPN meta-model with the relevant parameters will retain the properties of these layers, avoiding redundant verification. The proposed methods are currently adequate for verifying system determinism and deadlock freedom. The decomposition method introduced here can also serve as a basis for analyzing other properties in future studies.

Different causes of deadlocks: Section V discusses the analysis of properties for the RSHPN meta-model, with a focus on potential causes of deadlocks. While there are many possible causes, we highlight two key ones that should be considered when designing the RSHPN: (1) deadlocks occurring due to subsystem activities, where a lower-level

Petri net blocks the token and prevents it from reappearing in the higher-level network, and (2) inappropriate system initialization or incorrect selection of communication modes, such as the use of blocking communication (as in Fig. 14a).

The absence of a deadlock in an RSHPN (no global deadlock) does not mean that there is no local deadlock, i.e. that a subsystem or agent, or communication between several subsystems, is blocked by another agent/subsystem running in parallel. Consider the example shown in Fig. 14b, where there is a local deadlock (between subsystems A and B - bottom of Fig. 14b), while there is no global deadlock, i.e. there is always at least one transition in the network (in subsystem C) ready to fire, but the network models 3 subsystems running in parallel. It is therefore clear that the analysis methods we propose can be helpful in ensuring the correct operation of a robotic system.

Communication in multi-robot systems: In multi-robot systems, effective communication is of paramount importance to ensure proper coordination between subsystems. While this study focused on the analysis of blocking, non-blocking, and blocking with timeout communication modes, it is important to acknowledge that other aspects are equally significant, as evidenced by [24]. This is consistent with the findings of [26] concluding that there is a need for further investigation into the role of message content in multi-robotic communication. It is important to note that the content exchanged between agents depends on the specific task, and therefore cannot be generalised within the RSHPN meta-model, which is a generic template, i.e. the task is abstracted away.

Our approach, based on the RSHPN meta-model, allows not only 1-to-1 communication, but also 1-to-many communication, i.e. broadcasting, where receivers may be known or unknown to the sender. In cases where the receivers are unknown, communication takes place via stigmergy, where subsystems communicate indirectly via the environment. This is particularly relevant in swarm systems, where robots interact locally without direct coordination. In such cases, separate RSHPNs are constructed for each robot.

Modeling and analysis of multi-robot systems: For systems where many robots interact, it is possible to model their coordination either through separate RSHPNs or a single RSHPN with fused places that synchronize agents and subsystems. These systems can operate independently and activate their subsystems only when necessary, similar to processes running in an operating system. For example, in the ping-pong ball collecting robot system [15], a variable structure was used, allowing for the dynamic reconfiguration of subsystems.

Although RSHPN provides a framework for hierarchical coordination, individual agents can operate autonomously, without a central coordinator. Communication between agents can occur through direct exchange of information or through stigmergy, with no need for direct coordination. However, within individual agents, the control subsystem coordinates the activities of effectors and receptors to ensure the task is executed correctly.

The analysis of a single network modelling an entire multi-robot system consists in decomposing the network into layers and panels, and then performing network analysis for the

subsystem layer and the network modelling the communication arrangement layer (i.e. the communication model). In contrast, when analysing a system modelled with multiple networks, the analysis comes down to analysing networks for each individual robot and analysing the emergent interaction between robots. This requires the development of an additional Petri net. However, this is beyond the scope of this article. It focuses on the meta-model analysis, not on a specific class of systems for which the emergent behaviour is considered. However, swarm systems are an interesting area for future work.

IX. CONCLUSIONS

The RSHPN meta-model simplifies the verification of the correctness of a PN modelling the activities of a specific \mathcal{RS} . The meta-model serves as a template into which designed system specific parameters are inserted. The meta-model is thus transformed into a \mathcal{RS} model. This can be done using the RSSL language [16]. The RSHPN decomposition into 6 layers and the separation of panels defining PNs with one input and one output place avoid PN state space explosion and scalability issues. This enables network analysis to use reduction methods that collapse higher order networks into single transitions and lower order networks into single places, while preserving their properties. Key parts of the meta-model are general (e.g., behaviour layer PNs use the same pattern; multi-agent robotic systems and agent layers form trivial PNs) and are analysed once for all systems. Thus, the analysis of a specific \mathcal{RS} model is limited to a few PNs, such as subsystem layer PNs or communication and computation composition PNs. This allows designers to focus on analysing of the critical aspects of the system, such as the task definition and communication model. Modification of systems designed by using RSHPN is much easier (as indicated in [15], [16]), because of the modular structure only some subsystems need to be replaced, and therefore only new PNs need to be created and analysed.

Our motivation is to present a general meta-model that can be applied to the design of practically any robotic system, whether it is a single or multi-robot systems, with fixed or variable structures. In particular, the paper emphasises the formal analysis that can reveal system properties already in the specification phase. Verifying these properties prior to implementation is crucial, as it prevents costly errors that would otherwise be found during testing. Whilst the majority of PNs in the RSHPN meta-model satisfy the required properties, task-specific PNs should be developed according to the guidelines provided, offering significant value to system designers.

The PN analysis method in the future can be further extended to investigate additional \mathcal{RS} properties: (1) model checking (e.g.: schedulability, reachability [11], admissibility [25]) and (2) runtime verification (e.g.: task period and WCET overshoot [6]). Combining model checking with runtime verification, either by restricting the analysed state space [14] or by introducing predictive runtime verification [13] using the system model as *a priori* knowledge, would be beneficial. The RSHPN could be extended with constraints using Linear Temporal Logic (LTL) to introduce a supervisor

to monitor the system, as in [14], [25], and to propose tools to optimise system resources [27], mission, or tasks.

REFERENCES

- [1] S. García, et al., “Robotics Software Engineering: A Perspective from the Service Robotics Domain”. Association for Computing Machinery, p. 593–604, 2020.
- [2] E. de Araújo Silva, et al., “A survey of Model Driven Engineering in robotics”, *Journal of Computer Languages*, vol. 62, p. 101021, 2021.
- [3] S. Shivakumar, et al., “Soter on ROS: A run-time assurance framework on the Robot Operating System,” in *Runtime Verification*, Springer, 2020.
- [4] A. Ferrando, et al., “ROSMonitoring: A runtime verification framework for ROS,” in *Towards Autonomous Robotic Systems*, Springer, 2020.
- [5] J. Huang, et al., “ROSRV: Runtime verification for robots,” in *Runtime Verification*, Cham: Springer International Publishing, pp. 247–254, 2014.
- [6] S. Dal Zilio, P.-E. Hladik, F. Ingrand, and A. Mallet, “A formal toolchain for offline and run-time verification of robotic systems,” *Robotics and Autonomous Systems*, vol. 159, p. 104301, 2023.
- [7] “Robotics 2020 Multi-Annual Roadmap For Robotics in Europe - Horizon 2020 Call ICT-2017, SPARC The Partnership for Robotics in Europe: European Commission and euRobotics AISBL,” 2016.
- [8] S. Hustiu, C. Mahulea, M. Kloetzer, and J.-J. Lesage, “On multi-robot path planning based on Petri net models and ltl specifications,” *IEEE Transactions on Automatic Control*, pp. 1–8, 2024.
- [9] Z. He, J. Yuan, N. Ran, and X. Yin, “Security-based path planning of multi-robot systems by partially observed Petri nets and integer linear programming,” *IEEE Control Systems Letters*, vol. 8, pp. 352–357, 2024.
- [10] C. Lesire, D. Doose, and C. Grand, “Formalization of Robot Skills with Descriptive and Operational Models, in *2020 IEEE/RSJ International Conference on Intelligent Robots and Systems (IROS)*, pp. 7227–7232, 2020.
- [11] Y. Su, L. Qi, and M. Zhou, “A backward algorithm to determine the existence of legal firing sequences in ordinary Petri nets,” *IEEE Robotics and Automation Letters*, vol. 8, no. 6, pp. 3190–3197, 2023.
- [12] Z. Ding, et al., “Interactive-control-model for human–computer interactive system based on Petri nets,” *IEEE Transactions on Automation Science and Engineering*, vol. 16, no. 4, pp. 1800–1813, 2019.
- [13] S. Pinişetty, et al., “Predictive runtime verification of timed properties,” *Journal of Systems and Software*, vol. 132, pp. 353–365, 2017.
- [14] B. Pelletier, et al., “Predictive runtime verification of skill-based robotic systems using Petri nets,” in *2023 IEEE International Conference on Robotics and Automation (ICRA)*, pp. 10 580–10 586, 2023.
- [15] M. Figat and C. Zieliński, “Parameterised robotic system meta-model expressed by Hierarchical Petri nets,” *Robotics and Autonomous Systems*, vol. 150, p. 103987, 2022.
- [16] —, “Synthesis of robotic system controllers using Robotic System Specification Language,” *IEEE Robotics and Automation Letters*, vol. 8, no. 2, pp. 688–695, 2023.
- [17] M. Figat and C. Zieliński, “Robotic System Specification Methodology Based on Hierarchical Petri Nets,” *IEEE Access*, vol. 8, 2020.
- [18] “TINA (Time Petri Net Analyzer),” <https://projects.laas.fr/tina/news.php>.
- [19] R. Yang, et al., “Modeling and analysis of three properties of mobile interactive systems based on variable Petri nets,” *IEEE Transactions on Automation Science and Engineering*, vol. 20, no. 4, pp. 2479–2491, 2023.
- [20] M. Figat and C. Zieliński, “Methodology of designing multi-agent robot control systems utilising hierarchical Petri nets,” in *2019 International Conference on Robotics and Automation (ICRA)*, pp. 3363–3369, 2019.
- [21] T. Murata, “Petri nets: Properties, analysis and applications,” *Proceedings of the IEEE*, vol. 77, no. 4, pp. 541–580, 1989.
- [22] P. Freedman, “Time, Petri Nets, and Robotics,” *Robotics and Automation, IEEE Transactions on*, vol. 7, pp. 417 – 433, 1991.
- [23] W. Reisig, *Traps and Place Invariants of Generic System Nets*. Springer, pp. 119–129, 2013.
- [24] C. Zieliński, M. Figat, and R. Hexel, “Communication Within Multi-FSM Based Robotic Systems,” *Journal of Intelligent & Robotic Systems*, vol. 93, no. 3, pp. 787–805, Mar 2019.
- [25] B. Lacerda and P. U. Lima, “Petri net based multi-robot task coordination from temporal logic specifications,” *Robotics and Autonomous Systems*, vol. 122, p. 103289, 2019.
- [26] P. Pałka, et al., “Communication-focused top-down design of robotic systems based on binary decomposition,” *MDPI Energies*, vol. 15, no. 21, article no 7983, pp. 1187—1205, 2022.
- [27] M. Lahijanian, et al., “Resource-performance tradeoff analysis for mobile robots,” *IEEE Robotics and Automation Letters*, vol. 3, no. 3, pp. 1840–1847, 2018.